24th COBEM - 2017

24th ABCM International Congress of Mechanical Engineering
December 3-8, 2017, Curitiba, PR, Brazil

COBEM-2017-0196
MODELING AND CONTROL OF TANDEM COLD ROLLING MILLS

Alexandre Raider Leoni
José Adilson de Castro
Universidade Federal Fluminense, Programa de Pós-Graduação em Engenharia Mecânica, RJ, Brasil
alexandre.raider@gmail.com
joseadilsoncastro@id.uff.br

Péricles Guedes Alves
Instituto Federal de Educação Ciência e Tecnologia do Rio de Janeiro, RJ, Brasil
pericles.alves@ifrj.edu.br

Abstract. *The tandem cold rolling of metal strip is a complex, nonlinear multivariable process where the variables of each stand interact with each other, turning its control an engineering challenge. From the classic modeling base of the process, this study applies modern control techniques to improve the precision of the strip thickness control in an actual operation. The mathematical model was linearized for an effective use of the state space model and the process control was done using LQG (linear quadratic Gaussian control. Calculations and simulations were carried out using Matlab/Simulink and the results were compared with previous studies. After the first tests it was verified the need of the introduction of integral action for the exit strip thickness. The control model presented low values for overshoot, settling time and near null steady state error.*
Keywords: *tandem rolling, mathematical modeling, linearization, state space model, LQG control.*

1. INTRODUCTION

Tandem cold rolling is a metal working process whereby strip is deformed by successive rolling operations. Each rolling operation is achieved by squeezing the strip between a set of rolls. To achieve the required reduction and final tolerance for any given product several rolling operations will be required and this is done in tandem to achieve high production volumes (Geddes and Postlethwaite, 1994).

To improve the quality of the metal strip through its process control, this study aims to use the mathematical model developed by (Pittner and Simaan, 2011) and the modern control theory to project an optimal system to improve the precision and robustness of this control to disturbances. An optimal control must not only be efficient in computational simulation, but also overcome the common issues of a real process while obtaining good results with the usage of parameters of a real tandem cold rolling mill of five stands. A typical five-stand cold rolling mill is shown in Fig. 1.

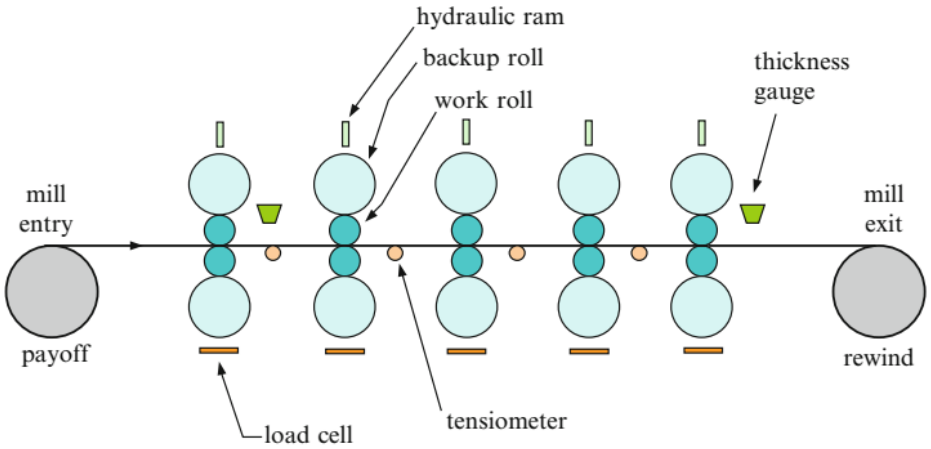

Figure 1. A typical five-stand cold rolling mill (Pittner and Simaan, 2011)

2. MATHEMATICAL MODELING

The equations are simplified forms of the classic derivations done by (Bryant, 1973), keeping important characteristics for controlling the tandem cold rolling mill, based on works by (Pittner *et al*., 2002) and (Alves *et al*., 2012).

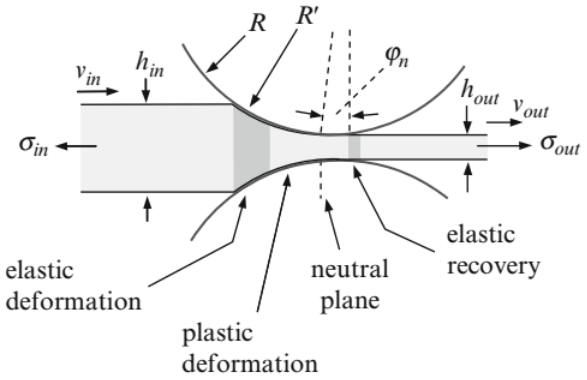

Figure 2. Roll bite area (Pittner and Simaan, 2011)

The strip deformation occurs in the roll bite area, as shown in Fig. 2, where the specific roll force is central to the development of a model for tandem cold rolling. The incoming strip is of thickness h_{in} at its centerline, under tension stress σ_{in} and is moving toward the roll bite with speed v_{in}. The strip exits the roll bite with thickness h_{out} at its centerline, under tension stress σ_{out} and with speed v_{out}. k_{in} is the compressive yield stress at the entry of the plastic zone and k_{out} at the exit. λ_1, λ_2 e λ_3 are constants of the strip material (Pittner and Simaan, 2011).

$$P = [\lambda_1 k_{in} + (1 - \lambda_1)k_{out} - \lambda_2\sigma_{in} + (1 - \lambda_2)\sigma_{out}](\sqrt{R'\delta})\left(1 + 0.4\sqrt{\frac{h_{out}}{h_{in}}}e^{\left(\frac{\mu\sqrt{R'\delta}}{\lambda_3 h_{in} + (1-\lambda_3)h_{out}}\right)} - 1\right) \tag{1}$$

During rolling, the work roll is elastically flattened from its radius R to a radius R'. This hypothesis is called Hitchcock's formula, shown in Eq. (2). E is Young's modulus e v is Poisson's ratio.

$$R' = R\left(1 + \frac{16(1 - v^2)P}{\pi E(h_{in} - h_{out})}\right) \tag{2}$$

The forward slip f, which is the percentage change increase of the strip speed at the roll bite exit in relation to the peripheral speed is shown in Eq. (3), where μ is the friction coefficient.

$$f = \left(\frac{h_{in} - h_{out}}{h_{out}}\right)\left(\frac{\frac{1}{2}\frac{h_{out}}{[\lambda_3 h_{in} + (1 - \lambda_3)h_{out}]}\sqrt{\frac{\delta}{R'}} - \frac{1}{4}\frac{h_{out}(h_{in} - h_{out})}{[\lambda_3 h_{in} + (1 - \lambda_3)h_{out})\mu R']} + \frac{1}{4}\frac{h_{out}}{\mu R'}\left[\frac{\sigma_{out}}{k_{out}} - \frac{\sigma_{in}}{k_{in}}\right]}{\sqrt{\left(\frac{h_{in} - h_{out}}{R'}\right)}}\right)^2 \tag{3}$$

By applying Hooke's law to a length of strip between successive mil stands, it is possible to develop an equation for interstand tension stress, applied over a time increment, as shown in Eq. (4), where L_0 is the distance between the rolling stands and i is the index related to the stand number.

$$\frac{d(\sigma_{i,i+1})}{dt} \equiv \dot{\sigma}_{i,i+1} = \frac{E(v_{in,i+1} - v_{out,i})}{L_0}, \quad \sigma_{i,i+1}(0) = \sigma_{0,i,i+1} \tag{4}$$

For the output thickness, a linear approximation was done, shown in Eq. (5), where S is the work roll actuator position, W is the strip width and M_m is the mil modulus.

$$h_{out} = S + \frac{PW}{M_m} \tag{5}$$

The time delay between stands $\tau_{d,i,i+1}$ is the time taken for a small element of strip to travel a distance L_0 from the exit of stand i to the entry of stand $i+1$.

$$\tau_{d,i,i+1} = \frac{L_0}{v_{out,i}} \tag{6}$$

The input thickness to stand 1 is the input thickness to the mill. The input thickness in a particular stand is the output thickness from the previous stand delayed by the interstand time delay.

$$h_{in,i}(t) = h_{out,i-1}(t - \tau_{d,i-1,i}) \tag{7}$$

The work roll actuator position controller is modeled as a single first order lag, just as the work roll drive speed controller, shown in Eq. (8) e (9) respectively, where V is the work roll peripheral speed, U_S is the position controller reference, τ_S is the actuator time constant, U_V is the drive speed reference and τ_V is the work roll speed time constant.

$$\dot{S} = \frac{U_S}{\tau_S} - \frac{S}{\tau_S}, \qquad S(0) = S_0 \tag{8}$$

$$\dot{V} = \frac{U_V}{\tau_V} - \frac{V}{\tau_V}, \qquad V(0) = V_0 \tag{9}$$

Considering the hypothesis of material continuity between adjacent stands and through the roll bite (Alves *et al*., 2012), the Eq. (10) and (11) can be obtained.

$$v_{out} = V(f + 1) \tag{10}$$

$$v_{in} = v_{out}\left(\frac{h_{out}}{h_{in}}\right) \tag{11}$$

3. LINEARIZATION AND STATE SPACE MODEL

To adequate the model for a state space model, a linearization of the govern equations are required. By applying a $\pm$5% variation around the operating points in process variables, a linear approximation of the mathematical model was developed in a similar process used by (Pittner *et al.*, 2002) and (Alves *et al.*, 2012). For the analytical analysis, Wolfram Mathematica was used instead of Matlab due to a better performance working with symbolical notation. The index i varies from 1 to 5, indicating the number of the rolling stand, with the index 0 showing the value at the operation point. Besides the linearization, the equations were normalized, utilizing its own value at the operation point, as shown in Eq. (12), considering a generic variable x.

$$\overline{\Delta x} = \frac{\Delta x}{x_0} = \frac{x - x_0}{x_0} \tag{12}$$

The specific roll force is dependent of the input and output strip thickness, of the input and output stress tensions, of the attrition coefficient and the strip material, but this study has not considered attrition and material variations. The linearized and normalized equation for the specific roll force is shown in Eq. (13), with its coefficients shown in Eq. (14) and (15).

$$\overline{\Delta P_i} = e_{2i}\overline{\Delta h}_{in,i} + (e_{1i} - 1)\overline{\Delta S}_i + e_{3i}\overline{\Delta\sigma}_{in,i} + e_{4i}\overline{\Delta\sigma}_{out,i} \tag{13}$$

$$e_{1i} = \frac{M_{mi}}{M_{mi} - \alpha_{2i}}\ ,\ e_{2i} = \frac{\alpha_{1i}h_{in,i0}}{h_{out,i0}(M_{mi} - \alpha_{2i})}\ ,\ e_{3i} = \frac{\alpha_{3i}\sigma_{in,i0}}{h_{out,i0}(M_{mi} - \alpha_{2i})}\ ,\ e_{4i} = \frac{\alpha_{4i}\sigma_{out,i0}}{h_{out,i0}(M_{mi} - \alpha_{2i})} \tag{14}$$

$$\alpha_{1i} = \left.\frac{\partial P_i}{\partial h_{in,i}}\right|_{PO}\ ,\ \alpha_{2i} = \left.\frac{\partial P_i}{\partial h_{out,i}}\right|_{PO}\ ,\ \alpha_{3i} = \left.\frac{\partial P_i}{\partial \sigma_{in,i}}\right|_{PO}\ ,\ \alpha_{4i} = \left.\frac{\partial P_i}{\partial \sigma_{out,i}}\right|_{PO} \tag{15}$$

The linearized and normalized equation for the output strip thickness is given by Eq. (16).

$$\overline{\Delta h}_{out,i} = e_{1i}\overline{\Delta S}_i + e_{2i}\overline{\Delta h}_{in,i} + e_{3i}\overline{\Delta\sigma}_{in,i} + e_{4i}\overline{\Delta\sigma}_{out,i} \tag{16}$$

Using the hypothesis presented at Eq. (11) and defining a relation between the forward slip and the backward slip, in addition to a partial derivation in Eq. (10) and (11), it was possible to come to a linearized and normalized equation that defines the forward slip, shown in Eq. (17) with its coefficients shown in Eq. (18).

$$\overline{\Delta f}_i^* = \beta_{1i}\overline{\Delta h}_{in,i} + \beta_{2i}\overline{\Delta h}_{out,i} + \beta_{3i}\overline{\Delta\sigma}_{in,i} + \beta_{4i}\overline{\Delta\sigma}_{out,i} \tag{17}$$

$$\beta_{1i} = \left.\frac{\partial f_i^*}{\partial h_{in,i}}\right|_{PO}, \quad \beta_{2i} = \left.\frac{\partial f_i^*}{\partial h_{out,i}}\right|_{PO}, \quad \beta_{3i} = \left.\frac{\partial f_i^*}{\partial \sigma_{in,i}}\right|_{PO}, \quad \beta_{4i} = \left.\frac{\partial f_i^*}{\partial \sigma_{out,i}}\right|_{PO} \tag{18}$$

By doing a partial derivation in Eq. (4) and substituting previous equations on the obtained derivative, it was possible to obtain all the equations for the interstand tensions and its coefficients, assuming that the variation at the output thickness and at the forward slip were null after the derivation. The linearized and normalized equations for the interstand tensions are shown in Eq. (19) to (22).

$$\frac{d}{dt}\overline{\Delta\sigma}_{in,12} = M_1\overline{\Delta\sigma}_{in,2} + M_2\overline{\Delta\sigma}_{in,3} + M_3\overline{\Delta h}_{in,1} + M_4\overline{\Delta V}_1 + M_5\overline{\Delta S}_1 + M_6\overline{\Delta h}_{in,2} + M_7\overline{\Delta V}_2 + M_8\overline{\Delta S}_2 + M_9\overline{\Delta\sigma}_{in,1} \tag{19}$$

$$\frac{d}{dt}\overline{\Delta\sigma}_{in,23} = N_1\overline{\Delta\sigma}_{in,2} + N_2\overline{\Delta\sigma}_{in,3} + N_3\overline{\Delta h}_{in,2} + N_4\overline{\Delta V}_2 + N_5\overline{\Delta S}_2 + N_6\overline{\Delta h}_{in,3} + N_7\overline{\Delta V}_3 + N_8\overline{\Delta S}_3 + N_9\overline{\Delta\sigma}_{in,4} \tag{20}$$

$$\frac{d}{dt}\overline{\Delta\sigma}_{in,34} = Q_1\overline{\Delta\sigma}_{in,3} + Q_2\overline{\Delta\sigma}_{in,4} + Q_3\overline{\Delta\sigma}_{in,5} + Q_4\overline{\Delta h}_{in,3} + Q_5\overline{\Delta h}_{in,4} + Q_6\overline{\Delta V}_3 + Q_7\overline{\Delta V}_4 + Q_8\overline{\Delta S}_3 + Q_9\overline{\Delta S}_4 \tag{21}$$

$$\frac{d}{dt}\overline{\Delta\sigma}_{in,45} = R_1\overline{\Delta\sigma}_{in,4} + R_2\overline{\Delta\sigma}_{in,5} + R_3\overline{\Delta h}_{in,4} + R_4\overline{\Delta h}_{in,5} + R_5\overline{\Delta V}_4 + R_6\overline{\Delta V}_5 + R_7\overline{\Delta S}_4 + R_8\overline{\Delta S}_5 + R_9\overline{\Delta\sigma}_{out,5} \tag{22}$$

For the actuators of positions and speed, the linearized and normalized equations are shown in Eq. (23) and (24), respectively.

$$\frac{d}{dt}\overline{\Delta S}_i = \frac{\overline{\Delta U}_{S_i}}{\tau_S} - \frac{\overline{\Delta S}_i}{\tau_S}, \qquad S_i(0) = 0 \tag{23}$$

$$\frac{d}{dt}\overline{\Delta V}_i = \frac{\overline{\Delta U}_{V_i}}{\tau_V} - \frac{\overline{\Delta V}_i}{\tau_V}, \qquad V_i(0) = 0 \tag{24}$$

The interstand time delay was approximated by a series of four first order lags, shown in Eq. (25), with n = 4.

$$e^{-\tau_d s} = \frac{1}{\left(\frac{\tau_d}{n}s + 1\right)^n} \tag{25}$$

The obtained linear model was represented in a state space model. Considering the disturbances and the uncertainties, its variables were represented by Eq. (26) and (27), with all its constant coefficients determined by the linear equations obtained previously by the linearization of the mathematical model. *A* is the system matrix, *B* is the control matrix, *C* is the output matrix, D_{in} is the input disturbances matrix and D_{out} is the output disturbances matrix. The state, output, control and disturbances vectors are shown in Eq. (28) to (31), respectively. The variables *q*, *r*, *z* and *a* are equations related to the interstand time delay.

$$\dot{x}(t) = Ax(t) + Bu(t) + D_{in}d, \qquad x(0) = 0 \tag{26}$$

$$y(t) = Cx(t) + D_{out}d \tag{27}$$

$$\mathrm{x} = \begin{bmatrix} \overline{\Delta\sigma}_{in,2} & \overline{\Delta\sigma}_{in,3} & \overline{\Delta\sigma}_{in,4} & \overline{\Delta\sigma}_{in,5} & \overline{\Delta h}_{in,1} & \overline{\Delta h}_{in,2} & \overline{\Delta h}_{in,3} & \overline{\Delta h}_{in,4} & \overline{\Delta h}_{in,5} & \overline{\Delta q}_{1} & \overline{\Delta q}_{2} & \overline{\Delta q}_{3} & \overline{\Delta r}_{1} \\ \overline{\Delta r}_{2} & \overline{\Delta r}_{3} & \overline{\Delta z}_{1} & \overline{\Delta z}_{2} & \overline{\Delta z}_{3} & \overline{\Delta a}_{1} & \overline{\Delta a}_{2} & \overline{\Delta a}_{3} & \overline{\Delta V}_{1} & \overline{\Delta V}_{2} & \overline{\Delta V}_{3} & \overline{\Delta V}_{4} & \overline{\Delta V}_{5} \\ \overline{\Delta S}_{1} & \overline{\Delta S}_{2} & \overline{\Delta S}_{3} & \overline{\Delta S}_{4} & \overline{\Delta S}_{5} \end{bmatrix}^{T} \quad (28)$$

$$\mathrm{y} = \begin{bmatrix} \overline{\Delta h}_{out,1} & \overline{\Delta h}_{out,2} & \overline{\Delta h}_{out,3} & \overline{\Delta h}_{out,4} & \overline{\Delta h}_{out,5} & \overline{\Delta\sigma}_{out,1} & \overline{\Delta\sigma}_{out,2} & \overline{\Delta\sigma}_{out,3} & \overline{\Delta\sigma}_{out,4} & \overline{\Delta P}_{1} & \overline{\Delta P}_{2} & \overline{\Delta P}_{3} \\ \overline{\Delta P}_{4} & \overline{\Delta P}_{5} \end{bmatrix}^{T} \quad (29)$$

$$\mathrm{u} = \begin{bmatrix} \overline{\Delta U}_{V_1} & \overline{\Delta U}_{V_2} & \overline{\Delta U}_{V_3} & \overline{\Delta U}_{V_4} & \overline{\Delta U}_{V_5} & \overline{\Delta U}_{S_1} & \overline{\Delta U}_{S_2} & \overline{\Delta U}_{S_3} & \overline{\Delta U}_{S_4} & \overline{\Delta U}_{S_5} \end{bmatrix}^{T} \quad (30)$$

$$\mathrm{d} = \begin{bmatrix} \overline{\Delta h}_{in,1} & \overline{\Delta\sigma}_{in,1} & \overline{\Delta\sigma}_{out,5} \end{bmatrix}^{T} \quad (31)$$

4. COMPUTACIONAL PROCEDURES

4.1 Model validation

The model was verified by simulation at Simulink, using three operation points shown in Table 1 and the parameters of the Table 2 from a benchmark cold rolling mill. It was applied disturbances at the entry thickness of the mill and at the tensions at the entry and exit of the mill. The effects on the output thickness, roll force and interstand tension were evaluated and compared with previous studies.

Table 1. Operational points used for validation

Parameters	*Operation points*		
	1	*2*	*3*
$h_{in,1}$(mm)	3.56	2.36	1.78
$h_{out,1}$(mm)	2.95	2.01	1.22
$h_{out,2}$(mm)	2.44	1.52	0.79
$h_{out,3}$(mm)	2.01	1.22	0.56
$h_{out,4}$(mm)	1.68	0.97	0.38
$h_{out,5}$(mm)	1.58	0.91	0.36
$\sigma_{in,1}$(kN/mm²)	0.0	0.0	0.0
$\sigma_{out,12}$(kN/mm²)	0.080	0.103	0.111
$\sigma_{out,23}$(kN/mm²)	0.078	0.126	0.132
$\sigma_{out,34}$(kN/mm²)	0.057	0.096	0.132
$\sigma_{out,45}$(kN/mm²)	0.055	0.060	0.085
$\sigma_{out,5}$(kN/mm²)	0.028	0.028	0.028

Table 2. Strip and material parameters

Parameter	*Dimension*
R (mm)	292
M_m (kN/mm)	3921
L_0 (mm)	4318
W (mm)	914
rh	1,095
E (kN/mm²)	207
μ	0,3
v	0,04
$v_{out,5}$ (m/s)	20,333
τ_S (s)	0,05
τ_V (s)	0,25

4.2 LQG control with integral action

The LQG control of the mill was done using the linear state space model, considering the process as stochastic and adding process and measure noises. Then the state estimator by Kalman filter was implemented, where the output vector is composed by the measurable outputs of the system, according to Eq. (32), where K is the optimal gain matrix and L is the gain matrix of the Kalman filter.

$$\dot{\hat{x}} = (A - BK - LC)\hat{x} + Ly \quad (32)$$

The estimated output vector is given by Eq. (33) and the control vector or estimated feedback vector is given by Eq. (34).

$$\hat{y} = C\hat{x} \quad (33)$$

$$u = -K\hat{x} \quad (34)$$

The performance index J used for control optimization is given by Eq. (35), where the output vector y and the controller vector u are weighted with the output matrix Q and the control matrix R.

$$J = \int_0^{\infty} (y^T Q y + u^T R u) dt \tag{35}$$

Optimal control and optimal state estimate feedback do not automatically introduce integral action, meaning that it has to be forced on the system. According to (Goodwin *et al*., 2000), one way of forcing integral action is to put a set of integrators at the output of the plant, as shown in Eq. (36).

$$\dot{z}(t) = -y(t) \tag{36}$$

The Kalman filter can be used to estimate x given u and y, assuming that x and z are directly measured. This can be written in state space form as a composite system as shown in Eq. (37) to (39).

$$\dot{x}'(t) = A'x(t) + B'u(t) \tag{37}$$

$$y(t) = C'x'(t) \qquad x'(t) = \begin{bmatrix} x(t) \\ z(t) \end{bmatrix} \tag{38}$$

$$A' = \begin{bmatrix} A & 0 \\ -C^* & 0 \end{bmatrix} \qquad B' = \begin{bmatrix} B \\ 0 \end{bmatrix} \qquad C' = \begin{bmatrix} C & \begin{matrix} 0 \\ \vdots \\ 0 \end{matrix} \\ & 1 \end{bmatrix} \tag{39}$$

The matrix C^* includes only the components that will receive integral action which, in case of study, equals to those corresponding to the output thickness at stand 5. The feedback matrix K of the Kalman filter must be established through the composite system as shown in Eq. (40).

$$\hat{\dot{x}} = (A - LC)\hat{x} - (BK)x' + Ly \tag{40}$$

The control law now utilizes the feedback matrix K obtained by the composite system and must contain the composite state vector as shown in Eq. (41).

$$u = -Kx' \tag{41}$$

A diagram of the Simulink model including the state space model and all control equations, Kalman filter, LQG control, step disturbances and the integral action at the output thickness of stand 5 is shown at Fig. 3.

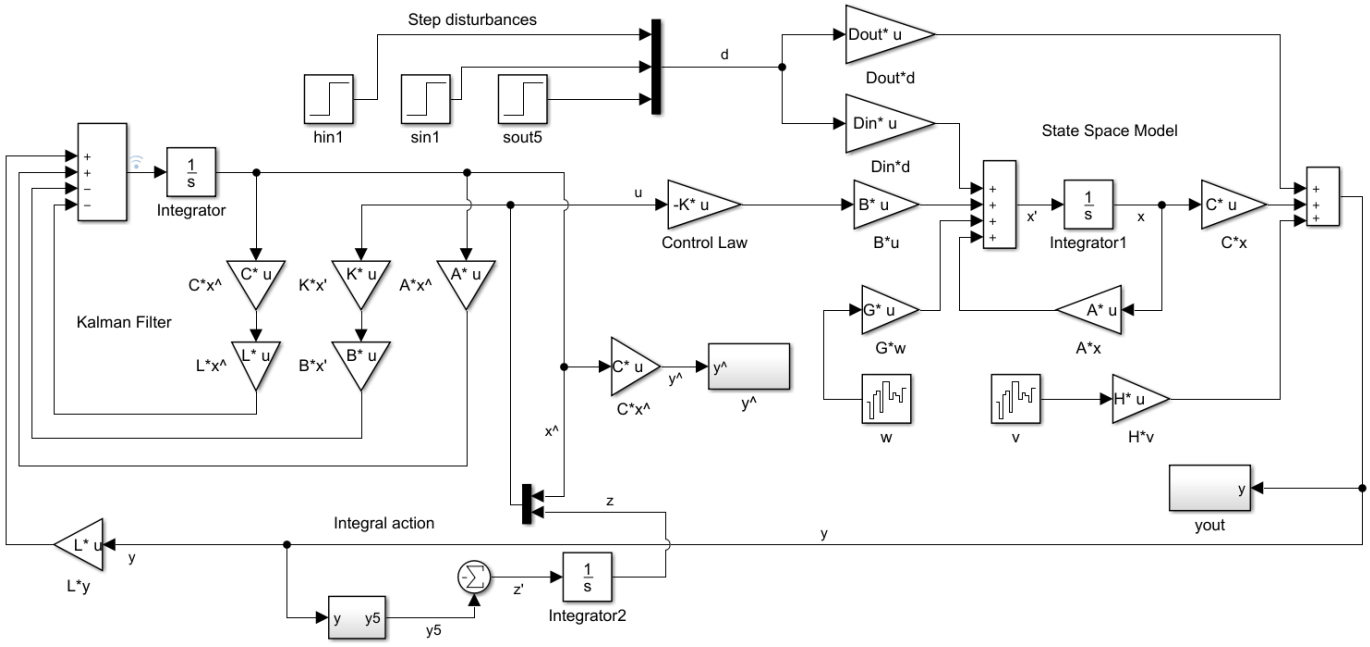

Figure 3. Simulink diagram of the LQG control with integral action

4.3 Real process parameters

The LQG control with integral action was implemented using parameters and operation points of a real cold rolling mill from a large company. This data is shown in Table 3 and 4 (Alves, 2013).

Table 3. Operation points of a real rolling process

Parameters	*Operation points*		
	400	*500*	*600*
$h_{in,1}$(mm)	4.750	4.750	4.750
$h_{out,1}$(mm)	3.903	3.904	3.903
$h_{out,2}$(mm)	3.284	3.284	3.284
$h_{out,3}$(mm)	2.829	2.829	2.829
$h_{out,4}$(mm)	2.492	2.492	2.492
$h_{out,5}$(mm)	2.480	2.480	2.480
$\sigma_{in,1}$(kN/mm²)	0.0127	0.0131	0.0133
$\sigma_{out,12}$(kN/mm²)	0.1089	0.1082	0.1084
$\sigma_{out,23}$(kN/mm²)	0.1136	0.1176	0.1162
$\sigma_{out,34}$(kN/mm²)	0.1188	0.1176	0.1188
$\sigma_{out,45}$(kN/mm²)	0.1240	0.1239	0.1247
$\sigma_{out,5}$(kN/mm²)	0.0263	0.0263	0.0263

Table 4. Parameters of a real rolling process

Parameter	*Dimension*
R_1 (mm)	279.913
R_2 (mm)	269.350
R_3 (mm)	255.600
R_4 (mm)	265.593
R_5 (mm)	263.593
M_m (kN/mm)	3925.5
L_0 (mm)	4600
W (mm)	1100
rh	1.095
E (kN/mm²)	200
μ	0.06
ν	0.3
$v_{out,5}$ (m/s)	8091
τ_S (s)	0.05
τ_V (s)	0.25

5. RESULTS AND DISCUSSION

5.1 Model validation

Table 3 shows the results obtained by the most recent studies by (Pittner and Simaan, 2011) and (Alves *et al*., 2012) in the validation test of the linear model. It features the average values obtained in each operating point after a step disturbance of 2% in the entry thickness of the mill at steady state. Analyzing the table, it can be noted that satisfactory values were obtained if comparing to previous studies, especially referring to interstand tension, and the results presented stable values throughout all stands. Therefore, the linear model is adequate for control implantation.

Table 5. Results of the model verification

Variable	*Source*	*Percent change in variable at steady state*				
		Stand 1	*Stand 2*	*Stand 3*	*Stand 4*	*Stand 5*
h_{out}	Pittner and Simaan	2.40	2.38	2.39	2.31	2.42
	Alves	1.702	1.47	1.448	1.132	1.122
	Model	1.576	1.505	1.500	1.489	1.468
P	Pittner and Simaan	2.17	1.67	1.35	1.09	1.57
	Alves	1.702	1.47	1.448	1.132	1.122
	Model	1.576	1.505	1.500	1.489	1.468
σ_{out}	Pittner and Simaan	1.2	0.7	0.4	8.8	-
	Alves	-5.15	-5.24	-4.59	-5.14	-
	Model	-2.922	-2.899	-3.593	-2.827	-

5.2 Control results

The simulation control was done in Simulink using the script developed in Matlab. Tests were done with the system out of its equilibrium position i.e. initial condition, meaning an increase of 10% in nominal values of the state variables of the process, in addition to an application of a step of disturbance in selected variables applied through the *d* vector, with 2% of magnitude. The red line indicates the real response of the system whereas the blue line indicates the estimated response given by the Kalman filter.

The control criteria were as follows: maximum overshoot of 25%, stabilization time inferior to 3 seconds and steady state error close to null for the output thickness at stand 5. Firstly, tests were done only with the LQG control, i.e. without integral action, but only the final and most important results will be shown.

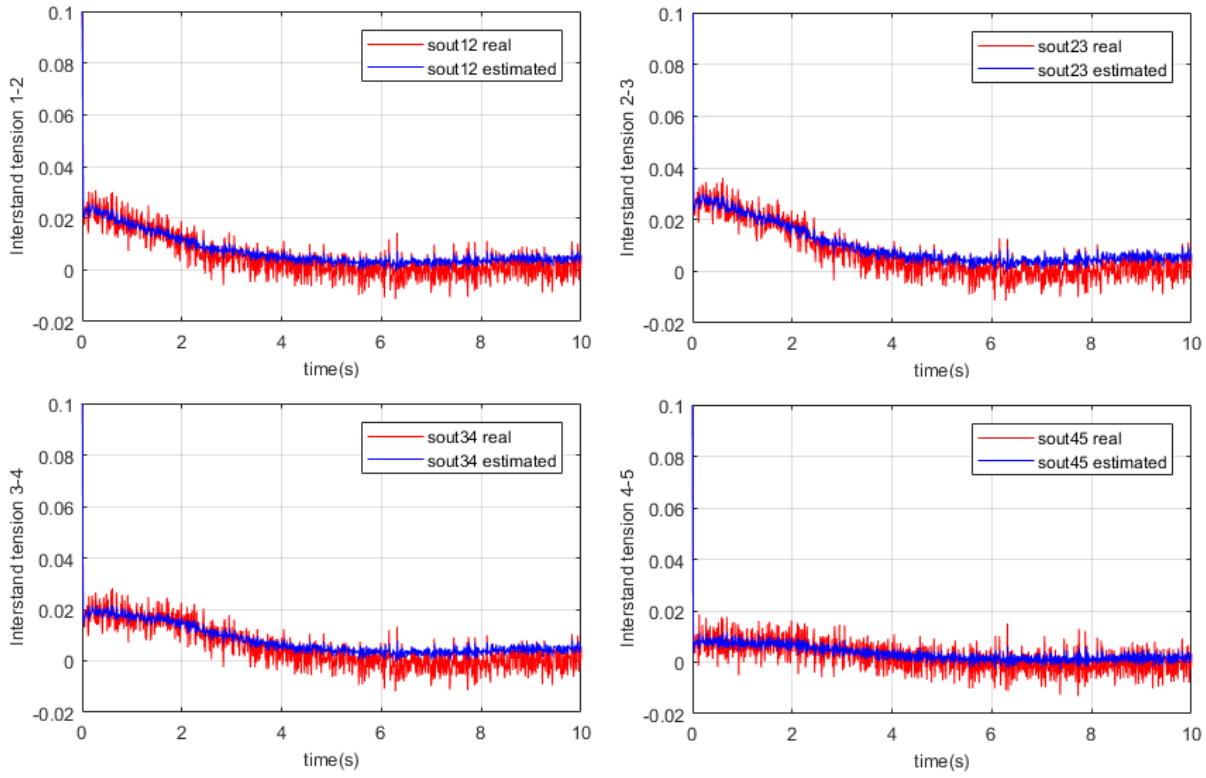

Figure 4. Control results for the interstand tensions

Control results for the interstand tensions are shown in Fig. 4. Despite the integral action being only at the output thickness at stand 5, it affects other variables of the system. The interstand tensions obtained high values of overshoot at the first instant, decaying rapidly after less than 0.1 second, showing that the integral action caused a high stabilization of the working forces at the system. The steady state error was very low, with averages between 0.022% and 0.303%, and the settling time was decreasing until getting closer to zero at the last stands.

The results for the roll force are shown in in Fig. 5. The integral action did not have a big impact in the system response, if comparing with the case without it. The steady state error at stand 1 was 2.468%, but decreased until 1.384% at stand 5. Settling time was under 3 seconds for all stands.

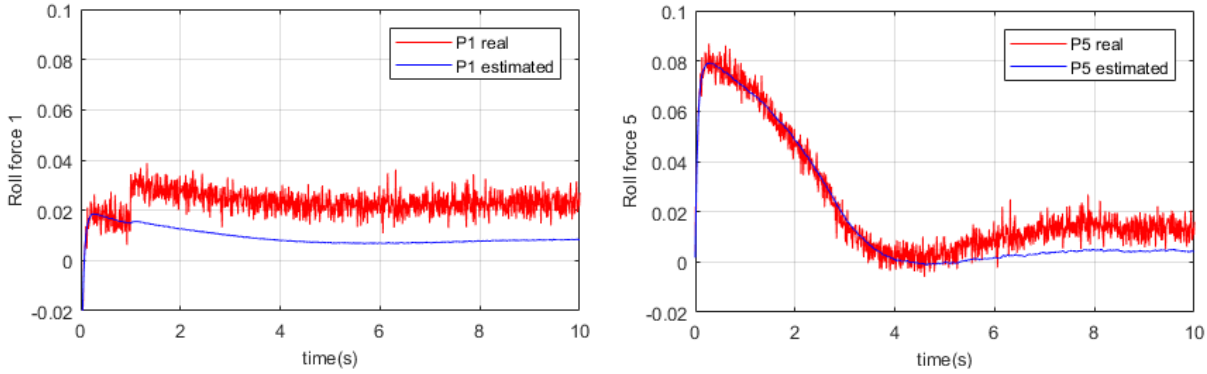

Figure 5. Control results for the roll force

The output thickness results are shown in Fig 6. The integral action almost eliminated the steady state error for the output thickness at stand 5, reaching an average value of 0.036% and still obtaining a good settling time of 2.6 seconds. Even though integral controllers are known for slowing down the system response, this was not the case. It is concluded that the control criteria were reached.

Table 6 shows overshoot values, settling time and the mean values for the steady state error with application of disturbances.

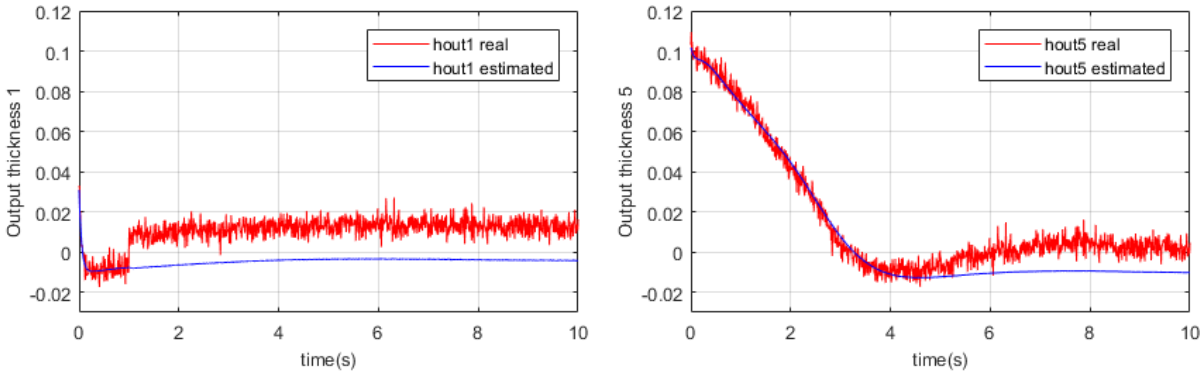

Figure 6. Control results for the output thickness

Table 6. Results of the LQG control with integral action

Variable	*Overshoot (%)*	*Settling Time (s)*(1)	*Steady state error (%)*(2)
$h_{out,1}$	4	1.0	1.210
$h_{out,5}$	11	2.6	0.036
P_1	4	1.0	2.468
P_2	6	1.3	1.659
P_3	7	2.0	1.492
P_4	7	2.4	1.020
P_5	6	2.8	1.384
$\sigma_{out,12}$	14	1.5	0.263
$\sigma_{out,23}$	20	2.0	0.303
$\sigma_{out,34}$	19	2.4	0.180
$\sigma_{out,45}$	16	0.1	0.022

(1) estimated using the 2% criteria
(2) measured by arithmetic mean between 10 and 50 seconds

6. CONCLUSIONS

The control model presented by this paper has shown great efficiency and big capacity for reduction of steady state error. The control criteria were reached, showing that the introduction of integral action to the LQG control improve considerably the final product quality without compromising the response time of the system. Besides, the linear state space model and the algorithm developed allows for further enhancement or even different control implantations due to its simplicity.

7. REFERENCES

Alves, P. G., Castro, J. A., Moreira, L. P., Hemerly, E. M., 2012. "Modeling, Simulation and Identification for Control of Tandem Cold Metal Rolling". Materials Research, São Carlos – S. P., Vol. 15, nº 6, pp 928-936.

Alves, P., G., 2013. *Modelagem e Controle de Laminadores Tandem de Tiras a Frio*. Doctoral Thesis. Universidade Federal Fluminense, Volta Redonda – RJ, Brazil.

Bryant, C. F., 1973. *Automation of Tandem Mills*. London: British Iron Steel Institute.

Geddes, E. J. M., Postlethwaite, I., 1998. "Improvements in Product Quality Cold Rolling Using Robust Multivariable Control". *IEEE Transactions on Control Systems Technology.* Vol. 6, n.º 2, pp. 257-269.

Goodwin, G. C., Graebe, S. F., Salgado, M. E., 2000. *Control System Design.* Valparaíso. 883p.

Pittner, J. and Simaan, M. A., 2011. *Tandem Cold Metal Rolling Mill Control – Using Practical Advanced Methods.* London: Springer-Verlag. 205p.

Pittner, J., Samaras, N. S., Simaan, M. A., 2002. A Simple Rolling Mill Model with Linear Quadratic Optimal Controller. IEEE Transactions on Industry Applications. pp. 142-149.

8. RESPONSIBILITY NOTICE

The authors are the only responsible for the printed material included in this paper.